

# UC Davis

## UC Davis Previously Published Works

### Title

Arterial Smooth Muscle Mitochondria Amplify Hydrogen Peroxide Microdomains Functionally Coupled to L-Type Calcium Channels

### Permalink

<https://escholarship.org/uc/item/0z22p9b9>

### Journal

Circulation Research, 117(12)

### ISSN

0009-7330

### Authors

Chaplin, Nathan L  
Nieves-Cintrón, Madeline  
Fresquez, Adriana M  
et al.

### Publication Date

2015-12-04

### DOI

10.1161/circresaha.115.306996

Peer reviewed



Published in final edited form as:

*Circ Res.* 2015 December 4; 117(12): 1013–1023. doi:10.1161/CIRCRESAHA.115.306996.

## Arterial Smooth Muscle Mitochondria Amplify Hydrogen Peroxide Microdomains Functionally Coupled to L-Type Calcium Channels

Nathan L. Chaplin<sup>1</sup>, Madeline Nieves-Cintrón<sup>2</sup>, Adriana M. Fresquez<sup>1</sup>, Manuel F. Navedo<sup>2</sup>, and Gregory C. Amberg<sup>1</sup>

<sup>1</sup>Department of Biomedical Sciences, Colorado State University, Fort Collins, CO 80523

<sup>2</sup>Department of Pharmacology, University of California, Davis, CA 95616

### Abstract

**Rationale**—Mitochondria are key integrators of convergent intracellular signaling pathways. Two important second messengers modulated by mitochondria are calcium and reactive oxygen species. To date, coherent mechanisms describing mitochondrial integration of calcium and oxidative signaling in arterial smooth muscle are incomplete.

**Objective**—To address and add clarity to this issue we tested the hypothesis that mitochondria regulate subplasmalemmal calcium and hydrogen peroxide microdomain signaling in cerebral arterial smooth muscle.

**Methods and Results**—Using an image-based approach we investigated the impact of mitochondrial regulation of L-type calcium channels on subcellular calcium and ROS signaling microdomains in isolated arterial smooth muscle cells. Our single cell observations were then related experimentally to intact arterial segments and to living animals. We found that subplasmalemmal mitochondrial amplification of hydrogen peroxide microdomain signaling stimulates L-type calcium channels and that this mechanism strongly impacts the functional capacity of the vasoconstrictor angiotensin II. Importantly, we also found that disrupting this mitochondrial amplification mechanism in vivo normalized arterial function and attenuated the hypertensive response to systemic endothelial dysfunction.

**Conclusions**—From these observations we conclude that mitochondrial amplification of subplasmalemmal calcium and hydrogen peroxide microdomain signaling is a fundamental mechanism regulating arterial smooth muscle function. As the principle components involved are fairly ubiquitous and positioning of mitochondria near the plasma membrane is not restricted to arterial smooth muscle, this mechanism could occur in many cell types and contribute to pathological elevations of intracellular calcium and increased oxidative stress associated with many diseases.

---

Address correspondence to: Dr. Gregory C. Amberg, Colorado State University, 1617 Campus Delivery, Fort Collins, CO 80523-1617, Tel: 970-491-4300, Fax: 970-491-7907, Gregory.Amberg@colostate.edu.

### DISCLOSURES

None.

## Keywords

Calcium sparklets; TIRF microscopy; hypertension; arterial smooth muscle; calcium channel

---

## INTRODUCTION

Mitochondria are central to eukaryotic aerobic metabolism. One consequence arising from the shuttling of electrons onto molecular oxygen during mitochondrial respiration is the formation of reactive oxygen species (ROS). Given the resultant necessity and subsequent ubiquity of ROS formation it is not surprising then that these generally toxic products of metabolism also function as purposeful second messenger molecules.<sup>1,2</sup>

Advances in cellular pathophysiology implicate mitochondrial dysfunction in the development and progression of illnesses including cancer,<sup>3</sup> neurodegeneration,<sup>4</sup> diabetes,<sup>5</sup> and cardiovascular disease.<sup>6,7</sup> As such, mitochondria are being evaluated as potential therapeutic targets for novel disease prevention and management strategies.<sup>8,9</sup> If mitochondria are to be viable therapeutic targets then a mechanistic understanding of mitochondrial function in multiple cell types is necessary to rationally predict and account for pharmacological responses to mitochondrial perturbations.

Here we investigated mitochondrial ROS signaling-dependent regulation of Ca<sup>2+</sup> influx in arterial smooth muscle. These cells are an ideal experimental model for this work due to their large surface area and because their geometry and morphological simplicity minimizes confounding variables possible in cells with more complex structural features. Furthermore, mitochondria, ROS, and Ca<sup>2+</sup> are each integral to arterial smooth muscle function and are thought to be involved in the development of cardiovascular disease.

Ca<sup>2+</sup>, as with ROS, is a ubiquitous signaling molecule that influences many processes ranging from contraction to gene expression. Ca<sup>2+</sup> and ROS as second messenger signaling molecules share at least four key attributes relevant to this study: First, Ca<sup>2+</sup> and ROS signaling events are known to be functionally coupled;<sup>10,11</sup> second, Ca<sup>2+</sup> and ROS signaling cascades attain specificity in part by subcellular compartmentalization;<sup>12,13</sup> third, Ca<sup>2+</sup> and ROS signaling events are influenced by mitochondria;<sup>10</sup> and fourth, Ca<sup>2+</sup> and ROS signaling cascades are implicated in the development of disease.<sup>11,14</sup>

In accordance with the first two attributes, our prior work showed that formation of punctate sites of ROS generation involving NADPH oxidase leads to colocalized Ca<sup>2+</sup> influx through L-type Ca<sup>2+</sup> channels.<sup>15–17</sup> We found that oxidative activation of protein kinase C (PKC),<sup>18</sup> which promotes localized Ca<sup>2+</sup> influx through L-type Ca<sup>2+</sup> channels,<sup>19–21</sup> functionally links Ca<sup>2+</sup> and ROS microdomain signaling in this context. Here we addressed the second pair of Ca<sup>2+</sup> and ROS signaling attributes listed above by investigating mitochondrial ROS-dependent regulation of arterial smooth muscle L-type Ca<sup>2+</sup> channels in relation to the development of hypertension-associated arterial dysfunction.

Experiments were performed on single cells, on excised arterial segments, and in living animals. Using this progressive subcellular in vitro-to-organismal in vivo approach we

conclude that amplification of hydrogen peroxide (H<sub>2</sub>O<sub>2</sub>) microdomain signaling by subplasmalemmal mitochondria promotes the opening of adjacent L-type Ca<sup>2+</sup> channels and subsequently the development of hypertension-associated arterial dysfunction.

## METHODS

Male Sprague-Dawley rats were euthanized with sodium pentobarbital (200 mg/kg intraperitoneally) as approved by the Institutional Animal Care and Use Committee of Colorado State University. Smooth muscle cells were isolated from basilar and cerebral arteries. Confocal microscopy was used to image the plasma membrane and mitochondria of single cells. L-type Ca<sup>2+</sup> channel sparklets and subplasmalemmal ROS were imaged with total internal reflection fluorescence (TIRF) microscopy.<sup>15,16</sup> Arterial diameters were recorded from middle cerebral arterial segments. Hypertension was induced in rats by including N<sup>o</sup>-nitro-L-arginine methyl ester (L-NAME) in their drinking water<sup>22-24</sup> and arterial blood pressure was monitored by telemetry as approved by the Institutional Animal Care and Use Committee of the University of California, Davis.

Normally distributed data are presented as the mean±standard error of the mean (SEM). To account for potential variability associated with cell isolation, all single myocyte experimental groups were comprised of cells obtained from 4 rats. Effect sizes, represented in the figures as bracketed values, are reported as Pearson's *r* (range -1.0 to 1.0; 0 indicates no effect);<sup>25,26</sup> *P* values <0.05 were considered significant. An expanded Materials and Methods section can be found in the Online Supplement at <http://circres.ahajournals.org>.

## RESULTS

### A subpopulation of mitochondria associates with the arterial smooth muscle cell plasma membrane at sites of elevated L-type Ca<sup>2+</sup> channel activity

To assess the subcellular distribution of mitochondria in arterial smooth muscle we marked the plasma membrane of cells with a wheat germ agglutinin conjugate (Alexa 555-WGA, red), labelled mitochondria with MitoTracker Green, and visualized the fluorescence with confocal microscopy (Figure 1A). We found that 8.64±0.42% of the total cell volume was occupied by mitochondria; this volume is consistent with prior reports.<sup>27</sup> While the majority of the MitoTracker signal was located centrally (>0.5 μm from the center of the Alexa 555-WGA signal), 7.50±0.77% of the mitochondrial volume was peripheral (<0.5 μm; yellow signal in Figure 1A, panel 3).

Next we examined MitoTracker-loaded cells with TIRF microscopy. Our images showed regions of MitoTracker fluorescence indicating the presence of subplasmalemmal mitochondria (Figure 2A, panel 1). Analysis of thresholded MitoTracker images revealed that only 3.29±0.26% (n=7 cells) of the visible plasma membrane was associated with mitochondria (Figure 2A, panel 2). We imaged Ca<sup>2+</sup> influx with a combination of TIRF microscopy and voltage-clamp electrophysiology.<sup>15,19,21</sup> This approach permits visualization of Ca<sup>2+</sup> influx through L-type Ca<sup>2+</sup> channels ("Ca<sup>2+</sup> sparklets"). To evoke Ca<sup>2+</sup> sparklets we exposed cells to angiotensin II (Ang II; 100 nM), which is known to promote mitochondrial ROS production.<sup>6</sup> Similar to our previous reports,<sup>15-17,28</sup> Ang II

induced L-type  $\text{Ca}^{2+}$  channel sparklet sites as revealed by localized changes in fluorescence of the  $\text{Ca}^{2+}$  indicator fluo-5F (Figure 2A, panel 3). The L-type  $\text{Ca}^{2+}$  channel sparklets induced by Ang II in this study were not different from the L-type  $\text{Ca}^{2+}$  channel sparklets observed previously in terms of quantal amplitude ( $36.2 \pm 3.2$  nmol/L [ $\text{Ca}^{2+}$ ]) and site densities and activities (see below).<sup>15–17</sup>

To visualize the spatial relationship between L-type  $\text{Ca}^{2+}$  channel activity and subplasmalemmal mitochondria we overlaid our fluo-5F and thresholded MitoTracker images (Figure 2A, panel 4). We then measured the distance from L-type  $\text{Ca}^{2+}$  channel sparklet site peaks (pixels of highest intensity) to the edge of the nearest MitoTracker signal and plotted the cumulative values (Figure 2B). Mitochondrial-associated L-type  $\text{Ca}^{2+}$  channel sparklet sites were defined *a priori* as those sites with peaks  $0.5 \mu\text{m}$  from the edge of the nearest thresholded MitoTracker signal; this is represented by the vertical dashed grey line in Figure 2B. We found that L-type  $\text{Ca}^{2+}$  channel function was associated with subplasmalemmal mitochondria (Figure 2B;  $n=5$  cells). The half-distance of the observed L-type  $\text{Ca}^{2+}$  channel sparklet sites ( $n=41$  sites) to the nearest mitochondria was  $0.43 \mu\text{m}$  (95% CI [0.39 to 0.47]) whereas the half-distance of 100 random points within the visible plasma membrane to the nearest mitochondria was  $2.10 \mu\text{m}$  (95% CI [1.99 to 2.19]).

Next we compared the activity of mitochondrial-associated (distance  $0.5 \mu\text{m}$ ) and non-associated L-type  $\text{Ca}^{2+}$  channel sparklet sites. L-type  $\text{Ca}^{2+}$  channel sparklet site activity can be expressed by the descriptor  $nP_s$ , where  $n$  is the number of quanta detected (i.e., number of functional channels) and  $P_s$  is the probability that the site is active.<sup>21</sup> Ang II-induced L-type  $\text{Ca}^{2+}$  channel sparklet sites associated with mitochondria were more active than those not associated with mitochondria (Figure 2C;  $P < 0.05$ ,  $r = 0.59$ ,  $n = 5$  cells). Indeed, mitochondrial-associated L-type  $\text{Ca}^{2+}$  channel sparklet sites accounted for  $\approx 73\%$  of the total  $\text{Ca}^{2+}$  sparklet activity observed. From these data we conclude that the spatial distribution of L-type  $\text{Ca}^{2+}$  channel activity is highly correlated with subplasmalemmal mitochondria.

### Mitochondrial-derived $\text{H}_2\text{O}_2$ stimulates L-type $\text{Ca}^{2+}$ channels

We reported previously that localized  $\text{H}_2\text{O}_2$  microdomains stimulate L-type  $\text{Ca}^{2+}$  channels in arterial smooth muscle via a PKC-dependent mechanism.<sup>15–17,20</sup> As mitochondria are a major source of ROS, we tested the hypothesis that localized  $\text{H}_2\text{O}_2$  generated by subplasmalemmal mitochondria stimulate nearby L-type  $\text{Ca}^{2+}$  channels.

To promote mitochondrial ROS generation we exposed cells to the electron transport chain complex III inhibitor antimycin (500 nmol/L).<sup>29,30</sup> First we investigated the effect of antimycin on subplasmalemmal ROS production with the fluorescent ROS indicator 5-(and-6)-chloromethyl-2',7'-dichlorodihydrofluorescein diacetate acetyl ester (DCF; 10  $\mu\text{mol/L}$ ) and monitored for changes in subplasmalemmal fluorescence (Figure 3A). Similar to Ang II,<sup>15,16</sup> antimycin induced localized sites of elevated DCF fluorescence (“ROS puncta”;<sup>15</sup> Figure 3A and B;  $P < 0.05$ ,  $r = 0.65$ ,  $n = 5$  cells); comparable ROS puncta formation was not apparent in time-matched controls. In contrast to the  $\approx 6$ -fold increase in DCF fluorescence associated with ROS puncta, the spatially averaged DCF fluorescence in cells treated with antimycin did not increase (Online Figure 1A;  $P > 0.05$ ;  $n = 5$  cells). This

observation is consistent with the concept of localized ROS generation by subplasmalemmal mitochondria.

Antimycin also induced localized L-type  $\text{Ca}^{2+}$  channel sparklets (Figure 3C and D). The L-type  $\text{Ca}^{2+}$  channel sparklet site activity ( $nP_s$ ;  $r=0.43$ ) and density (sites/ $\mu\text{m}^2$ ;  $r=0.75$ ) induced by antimycin was not different from that observed with Ang II (Figures 4C and 6D;  $P>0.05$ ,  $n=5$  cells).  $\text{Ca}^{2+}$  sparklet activity was not observed following antimycin treatment in cells pre-treated with nicardipine (10  $\mu\text{mol/L}$ ;  $P>0.05$ ;  $n=5$  cells, data not shown) or the PKC inhibitor Gö6976 (100 nmol/L; Online Figure IB and C). Similarly, dialyzing cells with catalase (500 U/mL) prevented the stimulatory effect of antimycin on L-type  $\text{Ca}^{2+}$  channels (Online Figure IB and C). These data are consistent with the hypothesis that antimycin-dependent promotion of localized mitochondrial  $\text{H}_2\text{O}_2$  generation stimulates neighboring L-type  $\text{Ca}^{2+}$  channels via a PKC-dependent mechanism.

Our previous work and results using the NADPH oxidase inhibitor ML171 (see Online Figure III) indicate that NADPH oxidase activity is necessary for local regulation of L-type  $\text{Ca}^{2+}$  channels by Ang II-induced  $\text{H}_2\text{O}_2$  microdomain signaling.<sup>15,16</sup> Ang II also induces mitochondrial ROS generation.<sup>6,31</sup> Therefore, we tested the effect of inhibiting mitochondrial ROS generation on Ang II-dependent stimulation of L-type  $\text{Ca}^{2+}$  channels.

The mitochondrial-targeted antioxidant mitoTEMPO attenuates the production of  $\text{H}_2\text{O}_2$  by mitochondria in response to Ang II.<sup>6,8,31,32</sup> We found that Ang II did not promote ROS puncta formation in cells pre-treated with mitoTEMPO (25 nmol/L for 15 min; Figure 4A and B;  $P>0.05$ ,  $r=-0.80$ ,  $n=5$  cells). MitoTEMPO also attenuated the stimulatory effect of Ang II on L-type  $\text{Ca}^{2+}$  channel sparklet site activity (Figure 4C and D;  $P>0.05$ ,  $r=-0.39$ ,  $n=5$  cells). Interestingly, and in contrast to NADPH oxidase inhibition or catalase,<sup>15,16</sup> mitoTEMPO did not prevent the increase in L-type  $\text{Ca}^{2+}$  channel sparklet site density (sites/ $\mu\text{m}^2$ ) induced by Ang II (Figure 4D;  $P<0.05$ ,  $r=-0.09$ ,  $n=5$  cells). MitoTEMPO did not have apparent nonspecific effects on macroscopic L-type  $\text{Ca}^{2+}$  channel currents (see Online Supporting Information *i*). These data suggest that in the presence of mitoTEMPO, Ang II-induced  $\text{Ca}^{2+}$  influx is minimal despite increasing the number of observed L-type  $\text{Ca}^{2+}$  channel sparklet sites. Similar results were observed when mitochondrial ROS production was limited with rotenone (see Online Supporting Information *ii*).

### Mitochondrial ROS production contributes to angiotensin II-mediated arterial contraction

L-type  $\text{Ca}^{2+}$  channels are the primary conduit for contractile  $\text{Ca}^{2+}$  in arterial smooth muscle.<sup>33</sup> As mitoTEMPO reduced Ang II-dependent stimulation of L-type  $\text{Ca}^{2+}$  channels we reasoned that inhibiting mitochondrial  $\text{H}_2\text{O}_2$  production with mitoTEMPO should decrease contractile responses to Ang II. To test this we applied Ang II to excised arterial segments pressurized to 60 mmHg. These experiments were performed in the presence of the nitric oxide synthase inhibitor  $N^G$ -nitro-L-arginine (L-NNA, 300  $\mu\text{mol/L}$ ) to prevent vasodilatory influences of endothelial-derived nitric oxide.

In control experiments Ang II constricted arteries to  $14.86\pm 0.99\%$  below their baseline diameter (Figure 5A). In arteries incubated with mitoTEMPO (1  $\mu\text{mol/L}$  for 15 min) Ang II induced a smaller contraction to only  $3.98\pm 0.99\%$  below baseline (Figure 5B;  $P<0.05$ ,  $r=$

–0.93, n=5 arteries). MitoTEMPO by itself had no apparent effect on baseline arterial constriction or the contractile response to 140 mmol/L KCl ( $P>0.05$ , n=3 arteries, data not shown). We reported previously that the non-targeted antioxidant TEMPOL does not suppress Ang II-dependent stimulation of L-type  $Ca^{2+}$  channels.<sup>16</sup> Therefore, we replicated our contractile experiments with Ang II on arteries incubated with TEMPOL (10  $\mu$ mol/L for 15 min). In contrast to mitoTEMPO, even at 10-fold higher concentration, TEMPOL did not reduce Ang II-dependent arterial constriction (Figure 5C and D;  $P>0.05$ ;  $r=-0.29$ , n=5 arteries). From these data we conclude that mitochondrial-derived ROS contribute to Ang II-dependent constriction of pressurized intact arterial segments.

### Reducing mitochondrial ROS production in vivo attenuates hypertensive arterial responses to endothelial dysfunction

To establish the importance of smooth muscle mitochondrial ROS production on arterial function *in vivo* we induced hypertension in rats by including the nitric oxide synthase inhibitor *N*<sup>ω</sup>-nitro-L-arginine methyl ester (L-NAME; 0.75 mg/mL) in their drinking water (dose  $\approx$ 50 mg/kg per day).<sup>22–24</sup> A key feature of L-NAME-induced hypertension is frank endothelial dysfunction and increased arterial constriction.<sup>34</sup> To examine the involvement of mitochondrial-derived ROS we infused L-NAME treated animals with mitoTEMPO at a rate of 150  $\mu$ g/kg per day<sup>8</sup> via subcutaneous osmotic minipumps; rats implanted with saline minipumps served as control. Arterial blood pressure was monitored by telemetry.

L-NAME induced a time-dependent increase in mean arterial pressure (Figure 6A;  $P<0.05$ ,  $r=0.98$ , n=5 rats). Similar to Ang II-induced hypertension,<sup>8</sup> co-administration of mitoTEMPO blunted ( $r=-0.72$ ) the hypertensive response to L-NAME (Figure 6B;  $P<0.05$ ,  $r=0.82$ , n=5 rats). The effect of mitoTEMPO on mean arterial pressure was evident on the third day of L-NAME treatment (Figure 6C  $P<0.05$ ,  $r=-0.96$ ). Thus, despite continued disruption of endothelial function, mitoTEMPO produced a modest decrease in blood pressure. This observation suggests that mitoTEMPO could be working *in vivo*, at least in part, by reducing mitochondrial ROS generation and subsequent stimulation of arterial smooth muscle L-type  $Ca^{2+}$  channels.

To investigate this we excised arterial segments from L-NAME and L-NAME plus mitoTEMPO treated animals and compared their myogenic set points (i.e., observed levels of myogenic tone). First we pressurized arteries to 20 mmHg and allowed them to equilibrate. Once a stable diameter was reached we increased the pressure to 60 mmHg and waited for an active myogenic contractile response to occur following passive dilation (Figure 6C). Experiments were terminated by superfusing the arteries with a nominally  $Ca^{2+}$ -free solution.

Arteries isolated from L-NAME treated animals infused with saline constricted robustly when the intraluminal pressure was increased from 20 to 60 mmHg ( $48.80\pm 2.06\%$  below passive diameter, n=5 arteries). Arteries from L-NAME treated animals infused with mitoTEMPO constricted substantially less following the same increase in pressure ( $30.43\pm 1.46\%$  below passive diameter,  $P<0.05$ ,  $r=-0.92$ , n=5 arteries). Note that arteries isolated from normotensive rats pressurized to 60 mmHg constricted to  $38.29\pm 3.20\%$  below their passive diameter (n=5 arteries) which was smaller than the constriction seen in arteries



from L-NAME treated animals infused with saline ( $P<0.05$ ) but not significantly different from the constriction seen in arteries from L-NAME treated animals infused with mitoTEMPO ( $P>0.05$ ). From these data we conclude that systemic inhibition of mitochondrial ROS generation with mitoTEMPO reduces L-NAME-induced arterial dysfunction in vivo (lowers systemic arterial pressure) and *ex vivo* (lowers arterial myogenic tone).

To investigate the mechanisms underlying mitoTEMPO-dependent preservation of arterial function we examined baseline ROS and  $\text{Ca}^{2+}$  microdomain signaling activity in cells isolated from these animals. Using DCF fluorescence as an indicator of ROS generation with TIRF microscopy, we found that ROS puncta density (in the absence of acute stimulation) was elevated in smooth muscle cells from hypertensive L-NAME treated rats compared to non-L-NAME-treated controls (Figure 7A and B;  $P<0.05$ ,  $r=0.70$ ,  $n=5$  cells). Importantly, ROS puncta densities in cells isolated from rats receiving L-NAME and mitoTEMPO were lower than those receiving L-NAME alone ( $P<0.05$ ,  $r=-0.74$ ,  $n=5$  cells). The ROS puncta density in these cells was negligible and not different from unstimulated control cells ( $P>0.05$ ,  $n=5$  cells).

Paralleling our ROS puncta data and consistent with previous observations in Ang II-induced and genetic hypertension,<sup>28</sup> basal L-type  $\text{Ca}^{2+}$  channel function was enhanced in cells isolated from hypertensive L-NAME treated rats as evidenced by elevated  $\text{Ca}^{2+}$  sparklet site activities and densities (Figure 7C and D;  $P<0.05$ ,  $nP_s$   $r=0.75$ , density  $r=0.64$ ,  $n=5$  cells). Notably, as with ROS puncta, mitoTEMPO infusion abolished L-NAME enhancement of L-type  $\text{Ca}^{2+}$  channel activity ( $P<0.05$ ,  $r=-0.51$ ,  $n=5$  cells) with levels not different from unstimulated cells from normotensive animals ( $P>0.05$ ,  $n=5$  cells). Taken altogether, we conclude that arterial smooth muscle mitochondrial-amplified  $\text{H}_2\text{O}_2$  microdomain signaling promotes  $\text{Ca}^{2+}$  influx through neighboring L-type  $\text{Ca}^{2+}$  channels and that this process contributes mechanistically to the contractile action of Ang II and the development of hypertension-associated arterial dysfunction.

## DISCUSSION

In this study we tested the hypothesis that mitochondrial amplification of  $\text{H}_2\text{O}_2$  microdomain signaling stimulates L-type  $\text{Ca}^{2+}$  channels in arterial smooth muscle. The major findings supporting this hypothesis are: 1) Subplasmalemmal mitochondria associate with sites of elevated L-type  $\text{Ca}^{2+}$  channel activity; 2) mitochondrial-derived  $\text{H}_2\text{O}_2$  stimulates  $\text{Ca}^{2+}$  influx through L-type channels; 3) inhibiting mitochondrial  $\text{H}_2\text{O}_2$  production reduces Ang II-mediated arterial contraction; and 4) inhibiting mitochondrial  $\text{H}_2\text{O}_2$  production attenuates the development of hypertension-associated arterial smooth muscle dysfunction *ex vivo* and *in vivo*. From these data we conclude that mitochondrial amplification of  $\text{H}_2\text{O}_2$  microdomain signaling is an important regulator of L-type  $\text{Ca}^{2+}$  channels in arterial smooth muscle and contributes to the development of hypertension-associated arterial dysfunction.

Our imaging of subplasmalemmal fluo-5F and MitoTracker fluorescence with TIRF microscopy provides compelling evidence that L-type  $\text{Ca}^{2+}$  channel activity is enriched at



areas of the plasma membrane associated with mitochondria (Figure 2). Consistent with this observation, the small amount of plasma membrane associated with mitochondria ( $\approx 5\%$ ) is sufficient to influence the surface area necessary ( $\approx 4\%$ ) to accommodate the L-type  $\text{Ca}^{2+}$  channel sparklet activity observed. This logic supports the conclusion that subcellular localization is a key factor in determining the stimulatory influence of mitochondria on L-type  $\text{Ca}^{2+}$  channels (see Online Supporting Information *iii*).

Evidence suggests that mitochondrial buffering of proximate  $\text{Ca}^{2+}$  flux events is an important mechanism by which these organelles influence  $\text{Ca}^{2+}$  signaling.<sup>35</sup> With respect to L-type  $\text{Ca}^{2+}$  channels, localized  $\text{Ca}^{2+}$  buffering by mitochondria could reduce the amplitude of the  $\text{Ca}^{2+}$  microdomain formed near the pore when the channel is open.<sup>36</sup> Lowering the effective  $\text{Ca}^{2+}$  concentration around the channel could alter  $\text{Ca}^{2+}$  signaling by reducing the  $\text{Ca}^{2+}$ -dependent inactivation characteristic of L-type  $\text{Ca}^{2+}$  channels.<sup>37</sup> Prior work in smooth muscle suggests that mitochondrial  $\text{Ca}^{2+}$  buffering does not influence  $\text{Ca}^{2+}$  influx through L-type  $\text{Ca}^{2+}$  channels.<sup>35,38</sup> However, our TIRF images demonstrate that L-type  $\text{Ca}^{2+}$  channel activity is associated with subplasmalemmal mitochondria (Figure 2). To reconcile these apparently contradictory observations we propose a mechanism of mitochondrial promotion of  $\text{Ca}^{2+}$  influx that does not rely on  $\text{Ca}^{2+}$  buffering *per se*. Rather, we propose that mitochondria promote  $\text{Ca}^{2+}$  influx by amplifying  $\text{H}_2\text{O}_2$  microdomain signaling in the vicinity of L-type  $\text{Ca}^{2+}$  channels which leads to oxidant-dependent stimulation of  $\text{Ca}^{2+}$  influx.<sup>15-17</sup>

Functionally compartmentalized submembranous accumulation of  $\text{H}_2\text{O}_2$  is thought to bring about competent  $\text{H}_2\text{O}_2$  signaling microdomains.<sup>39</sup> We reported previously that  $\text{H}_2\text{O}_2$  microdomains involving NADPH oxidase promote colocalized  $\text{Ca}^{2+}$  influx through L-type  $\text{Ca}^{2+}$  channels via oxidative activation of PKC.<sup>15-17</sup> Experiments in this study provide evidence indicating that peripheral mitochondria also participate in  $\text{H}_2\text{O}_2$  microdomain-dependent stimulation of L-type  $\text{Ca}^{2+}$  channels. Antimycin induced the formation of subplasmalemmal ROS puncta and induced L-type  $\text{Ca}^{2+}$  channel sparklet activity. Lastly, antimycin-dependent stimulation of L-type  $\text{Ca}^{2+}$  channels was abolished by enhanced decomposition of  $\text{H}_2\text{O}_2$  with intracellular catalase.

To specifically reduce the influence of mitochondrial ROS on L-type  $\text{Ca}^{2+}$  channels we used the mitochondrial-targeted antioxidant mitoTEMPO at a concentration where cytosolic antioxidant effects are not apparent.<sup>6,8,31</sup> MitoTEMPO prevented the induction of ROS puncta formation by Ang II and reduced the stimulatory effect on L-type  $\text{Ca}^{2+}$  channel sparklets. This suggests that mitochondrial ROS (visualized as ROS puncta) stimulate L-type  $\text{Ca}^{2+}$  channels. Intriguingly, unlike the effect on  $\text{Ca}^{2+}$  sparklet activity, mitoTEMPO did not reduce the effect of Ang II on L-type  $\text{Ca}^{2+}$  channel sparklet density (sites/ $\mu\text{m}^2$ ). This is in contrast to the effects of NADPH oxidase inhibition and catalase on Ang II-dependent L-type  $\text{Ca}^{2+}$  channel sparklets where activity and density are reduced.<sup>15,16</sup> While initially perplexing, we believe this subtle observation provides valuable mechanistic insight into the signaling events underlying oxidant-dependent regulation of L-type  $\text{Ca}^{2+}$  channels. Activation of Ang II type 1 receptors stimulates NADPH oxidase resulting in ROS formation.<sup>40,41</sup> Evidence suggests that ROS produced by NADPH oxidase can induce subsequent ROS generation from mitochondria through the process of ROS-induced ROS

release (RIRR).<sup>8,31,32</sup> We suggest that a ROS-induced ROS release mechanism, initiated by NADPH oxidase and carried out by proximate mitochondria, is essential for Ang II-dependent stimulation of L-type  $\text{Ca}^{2+}$  channels in arterial smooth muscle.

This hypothesis is compatible with our data. Disrupting Ang II signaling by NADPH oxidase inhibition or enhancing  $\text{H}_2\text{O}_2$  decomposition with catalase reduces the initial availability of signaling  $\text{H}_2\text{O}_2$  and abolishes the stimulatory effect of Ang II on L-type  $\text{Ca}^{2+}$  channel sparklets (i.e., activity and density).<sup>15,16</sup> However, mitoTEMPO impairment of  $\text{H}_2\text{O}_2$  generation occurs further along the signaling cascade by limiting ROS-induced ROS release by mitochondria. Thus, the initial production of signaling  $\text{H}_2\text{O}_2$  by NADPH oxidase remains intact which could trigger limited stimulation of L-type  $\text{Ca}^{2+}$  channels leading to an increase in low-activity L-type  $\text{Ca}^{2+}$  channel sparklet sites. From this we suggest that mitochondria, as a consequence of providing a means of ROS-induced ROS release, function as amplifiers of NADPH oxidase-initiated  $\text{H}_2\text{O}_2$  microdomain signaling and that this mechanism is necessary for physiological stimulation of arterial smooth muscle cell L-type  $\text{Ca}^{2+}$  channels by Ang II (Figure 7E).

If mitochondrial ROS-induced ROS release is necessary for physiological stimulation of L-type  $\text{Ca}^{2+}$  channels by Ang II then disrupting this process with mitoTEMPO should reduce arterial contractile responses to Ang II. Consistent with this, mitoTEMPO reduced Ang II-dependent contraction of pressurized cerebral arteries by  $\approx 70\%$ . In contrast, MitoTEMPO had no effect on the baseline myogenic tone of these arteries. Similarly, we noted previously that inhibition of NADPH oxidase<sup>15</sup> and application of cell-permeable catalase<sup>16</sup> reduced contractile responses to Ang II without altering arterial tone. These observations suggest that, at least in cerebral arteries from healthy rats,  $\text{H}_2\text{O}_2$  microdomain stimulation of smooth muscle L-type  $\text{Ca}^{2+}$  channels contributes to the vasoconstrictor capacity of Ang II but does not influence baseline myogenic function.

In contrast to our observations, work by others has shown that mitochondrial and NADPH oxidase-derived ROS reduce arterial contractility by enhancing activation of hyperpolarizing large-conductance,  $\text{Ca}^{2+}$ -activated potassium (BK) channels.<sup>42,43</sup> We contend that our  $\text{H}_2\text{O}_2$  microdomain signaling hypothesis reconciles these seemingly diametrically opposed observations. In the case of our data,  $\text{H}_2\text{O}_2$  microdomain signaling is coupled to the activation of L-type  $\text{Ca}^{2+}$  channels leading to contraction. For vasodilatory-associated ROS, we hypothesize that discrete ROS signaling events are selectively coupled to vasodilatory processes. In addition, we hypothesize that ROS microdomain signaling attains differential coupling specificity as a consequence of distinct subcellular distribution patterns inherent to the underlying ROS generating mechanisms (see Online Supporting Information *iv*).

Anomalous Ang II signaling is implicated in the development of arterial dysfunction and hypertension.<sup>6,32,44</sup> We found that mitoTEMPO attenuated the vasoconstrictive capacity of Ang II and, conversely, that stimulating mitochondrial ROS production with antimycin increased L-type  $\text{Ca}^{2+}$  channel activity. We therefore examined the efficacy of mitoTEMPO in mitigating arterial smooth muscle dysfunction in hypertension. Systemic administration of mitoTEMPO blunts the hypertensive response to Ang II infusion in mice, at least in part, by increasing the bioavailability of nitric oxide and preserving endothelial function.<sup>8</sup> To

investigate the effect of mitoTEMPO on arterial smooth muscle function we used a nitric oxide-deficient model of hypertension where endothelial dysfunction is an etiological hallmark.<sup>34,45</sup> Similar to Ang II infusion,<sup>8</sup> co-administration of mitoTEMPO reduced the hypertensive response to L-NAME. This observation suggests that the antihypertensive effect of mitoTEMPO reside, at least in part, at the level of arterial smooth muscle.

To examine the effect of systemically administered mitoTEMPO on arterial smooth muscle function we isolated and pressurized cerebral arteries obtained from L-NAME-treated rats. Arteries from these rats contracted to  $\approx 50\%$  below their passive diameter when pressurized to 60 mmHg. In contrast, arteries from L-NAME-treated rats infused with mitoTEMPO contracted to only  $\approx 30\%$  below their passive diameter. For perspective, the control arteries used in our Ang II/mitoTEMPO experiments contracted to  $\approx 38\%$  below their passive diameter, which was not significantly different from that seen with mitoTEMPO. Thus, systemically administered mitoTEMPO normalized the intrinsic myogenic set point of arteries isolated from L-NAME-treated rats.

To investigate the mechanisms by which mitoTEMPO normalized arterial function in L-NAME-treated rats we examined L-type  $\text{Ca}^{2+}$  channel and  $\text{H}_2\text{O}_2$  microdomain signaling in isolated cells. Similar to Ang II-dependent and genetic hypertension,<sup>28</sup> basal L-type  $\text{Ca}^{2+}$  channel sparklet activity and ROS puncta density were elevated in cells from hypertensive L-NAME-treated rats. Strikingly, arterial smooth muscle cells isolated from rats infused with mitoTEMPO showed no increase in either ROS puncta density or L-type  $\text{Ca}^{2+}$  channel sparklet activity. From these data we conclude that mitoTEMPO preserves arterial function and reduces arterial blood pressure, at least in part, by inhibiting mitochondrial amplified  $\text{H}_2\text{O}_2$  microdomain dependent stimulation of arterial smooth muscle L-type  $\text{Ca}^{2+}$  channels.

The implications of our observations are broad. First, we suggest that mitochondrial amplification of  $\text{H}_2\text{O}_2$  microdomain signaling in arterial smooth muscle is a potentially viable therapeutic target for reducing hypertension-associated arterial dysfunction. Second, as mitochondria and L-type  $\text{Ca}^{2+}$  channels are widely distributed we suggest that localized mitochondrial amplification of  $\text{H}_2\text{O}_2$  microdomain signaling could be a general mechanism for promoting  $\text{Ca}^{2+}$  influx through L-type  $\text{Ca}^{2+}$  channels in many cell types including cardiac myocytes as demonstrated by others.<sup>46–48</sup> Indeed, we recently described a mechanism responsible for localized L-type  $\text{Ca}^{2+}$  channel function in neuroendocrine pituitary gonadotrope cells which bears a striking resemblance to our observations in smooth muscle<sup>49</sup> Lastly, this mechanism could be an important factor contributing to the exaggerated ROS production and  $\text{Ca}^{2+}$  influx associated with the pathogenesis of numerous cardiovascular and non-cardiovascular diseases.

## Supplementary Material

Refer to Web version on PubMed Central for supplementary material.

## Acknowledgments

We thank Dr. Chao-Yin Chen for the use of the telemetry system.

## SOURCES OF FUNDING

This work was supported by the National Institute of Health Grants 1R01HL111060 (to GCA) and 1R01HL098200 and 1R01HL121059 (to MNF), the American Heart Association (14GRNT18730054; to MNF), the Colorado State University College Research Council (to GCA), and the Pew Charitable Trusts (to GCA).

## Nonstandard Abbreviations and Acronyms

<b>Ang II</b>	angiotensin II
<b>DCF</b>	5-(and-6)-chloromethyl-2'7'-dichlorodihydrofluorescein diacetate acetyl ester
<b>L-NAME</b>	<i>N</i> <sup>o</sup> -nitro-L-arginine methyl ester
<b>L-NNA</b>	<i>N</i> <sup>o</sup> -nitro-L-arginine
<b>PKC</b>	protein kinase C
<b>ROS</b>	reactive oxygen species
<b>RIRR</b>	ROS-induced ROS release
<b>TIRF</b>	total internal reflection fluorescence

## References

1. Clempus RE, Griendling KK. Reactive oxygen species signaling in vascular smooth muscle cells. *Cardiovascular research*. 2006; 71:216–225. [PubMed: 16616906]
2. Hool LC. Reactive oxygen species in cardiac signalling: From mitochondria to plasma membrane ion channels. *Clin Exp Pharmacol Physiol*. 2006; 33:146–151. [PubMed: 16445714]
3. Lynam-Lennon N, Maher SG, Maguire A, Phelan J, Muldoon C, Reynolds JV, O'Sullivan J. Altered mitochondrial function and energy metabolism is associated with a radioresistant phenotype in oesophageal adenocarcinoma. *PLoS One*. 2014; 9:e100738. [PubMed: 24968221]
4. Gonzalez-Lima F, Barksdale BR, Rojas JC. Mitochondrial respiration as a target for neuroprotection and cognitive enhancement. *Biochem Pharmacol*. 2014; 88:584–593. [PubMed: 24316434]
5. Peinado JR, Ruiz AD, Frühbeck G, Malagon MM. Mitochondria in metabolic disease. Getting clues from proteomic studies. *Proteomics*. 2013
6. Dikalov SI, Nazarewicz RR. Angiotensin II-induced production of mitochondrial reactive oxygen species: Potential mechanisms and relevance for cardiovascular disease. *Antioxid Redox Signal*. 2012
7. Serpillon S, Floyd BC, Gupte RS, George S, Kozicky M, Neito V, Recchia F, Stanley W, Wolin MS, Gupte SA. Superoxide production by NAD(P)H oxidase and mitochondria is increased in genetically obese and hyperglycemic rat heart and aorta before the development of cardiac dysfunction. The role of glucose-6-phosphate dehydrogenase-derived NADPH. *Am J Physiol Heart Circ Physiol*. 2009; 297:H153–162. [PubMed: 19429815]
8. Dikalova AE, Bikineyeva AT, Budzyn K, Nazarewicz RR, McCann L, Lewis W, Harrison DG, Dikalov SI. Therapeutic targeting of mitochondrial superoxide in hypertension. *Circ Res*. 2010; 107:106–116. [PubMed: 20448215]
9. Rao VK, Carlson EA, Yan SS. Mitochondrial permeability transition pore is a potential drug target for neurodegeneration. *Biochim Biophys Acta*. 2014; 1842:1267–1272. [PubMed: 24055979]
10. Feissner RF, Skalska J, Gaum WE, Sheu SS. Crosstalk signaling between mitochondrial Ca<sup>2+</sup> and ROS. *Front Biosci*. 2009; 14:1197–1218.
11. Hidalgo C, Donoso P. Crosstalk between calcium and redox signaling: From molecular mechanisms to health implications. *Antioxid Redox Signal*. 2008; 10:1275–1312. [PubMed: 18377233]
12. Berridge MJ, Lipp P, Bootman MD. The versatility and universality of calcium signalling. *Nat Rev Mol Cell Biol*. 2000; 1:11–21. [PubMed: 11413485]

13. Terada LS. Specificity in reactive oxidant signaling: Think globally, act locally. *The Journal of cell biology*. 2006; 174:615–623. [PubMed: 16923830]
14. Hool LC. Evidence for the regulation of L-type  $\text{Ca}^{2+}$  channels in the heart by reactive oxygen species: Mechanism for mediating pathology. *Clin Exp Pharmacol Physiol*. 2008; 35:229–234. [PubMed: 18197892]
15. Amberg GC, Earley S, Glapa SA. Local regulation of arterial L-type calcium channels by reactive oxygen species. *Circ Res*. 2010; 107:1002–1010. [PubMed: 20798361]
16. Chaplin NL, Amberg GC. Hydrogen peroxide mediates oxidant-dependent stimulation of arterial smooth muscle L-type calcium channels. *American journal of physiology. Cell physiology*. 2012; 302:C1382–1393. [PubMed: 22322977]
17. Chaplin NL, Amberg GC. Stimulation of arterial smooth muscle L-type calcium channels by hydrogen peroxide requires protein kinase C. *Channels (Austin)*. 2012; 6:385–389. [PubMed: 22907102]
18. Knapp LT, Klann E. Superoxide-induced stimulation of protein kinase C via thiol modification and modulation of zinc content. *The Journal of biological chemistry*. 2000; 275:24136–24145. [PubMed: 10823825]
19. Amberg GC, Navedo MF, Nieves-Cintrón M, Molkentin JD, Santana LF. Calcium sparklets regulate local and global calcium in murine arterial smooth muscle. *J Physiol*. 2007; 579:187–201. [PubMed: 17158168]
20. Navedo MF, Amberg GC. Local regulation of L-type  $\text{Ca}^{2+}$  channel sparklets in arterial smooth muscle. *Microcirculation*. 2013; 20:290–298. [PubMed: 23116449]
21. Navedo MF, Amberg GC, Votaw VS, Santana LF. Constitutively active L-type  $\text{Ca}^{2+}$  channels. *Proc Natl Acad Sci U S A*. 2005; 102:11112–11117. [PubMed: 16040810]
22. Takemoto M, Egashira K, Usui M, Numaguchi K, Tomita H, Tsutsui H, Shimokawa H, Sueishi K, Takeshita A. Important role of tissue angiotensin-converting enzyme activity in the pathogenesis of coronary vascular and myocardial structural changes induced by long-term blockade of nitric oxide synthesis in rats. *J Clin Invest*. 1997; 99:278–287. [PubMed: 9005996]
23. Bartunek J, Weinberg EO, Tajima M, Rohrbach S, Katz SE, Douglas PS, Lorell BH. Chronic  $\text{N}^{\text{G}}$ -nitro-L-arginine methyl ester-induced hypertension: Novel molecular adaptation to systolic load in absence of hypertrophy. *Circulation*. 2000; 101:423–429. [PubMed: 10653835]
24. Lu Y, Zhang H, Gokina N, Mandala M, Sato O, Ikebe M, Osol G, Fisher SA. Uterine artery myosin phosphatase isoform switching and increased sensitivity to SNP in a rat L-NAME model of hypertension of pregnancy. *American journal of physiology. Cell physiology*. 2008; 294:C564–571. [PubMed: 18094148]
25. Cohen, J. *Statistical power analysis for the behavioral sciences*. Hillsdale, N.J: L. Erlbaum Associates; 1988.
26. Rosenthal R, Rubin DB. R equivalent: A simple effect size indicator. *Psychol Methods*. 2003; 8:492–496. [PubMed: 14664684]
27. Somlyo AP. Excitation-contraction coupling and the ultrastructure of smooth muscle. *Circ Res*. 1985; 57:497–507. [PubMed: 3899402]
28. Nieves-Cintrón M, Amberg GC, Navedo MF, Molkentin JD, Santana LF. The control of  $\text{Ca}^{2+}$  influx and NFATc3 signaling in arterial smooth muscle during hypertension. *Proc Natl Acad Sci U S A*. 2008; 105:15623–15628. [PubMed: 18832165]
29. Murphy MP. How mitochondria produce reactive oxygen species. *The Biochemical journal*. 2009; 417:1–13. [PubMed: 19061483]
30. Zorov DB, Juhaszova M, Sollott SJ. Mitochondrial reactive oxygen species (ROS) and ROS-induced ROS release. *Physiol Rev*. 2014; 94:909–950. [PubMed: 24987008]
31. Dikalov S. Cross talk between mitochondria and NADPH oxidases. *Free Radic Biol Med*. 2011; 51:1289–1301. [PubMed: 21777669]
32. Dikalov SI, Ungvari Z. Role of mitochondrial oxidative stress in hypertension. *Am J Physiol Heart Circ Physiol*. 2013; 305:H1417–1427. [PubMed: 24043248]
33. Knot HJ, Nelson MT. Regulation of arterial diameter and wall  $[\text{Ca}^{2+}]$  in cerebral arteries of rat by membrane potential and intravascular pressure. *J Physiol*. 1998; 508:199–209. [PubMed: 9490839]

34. Paulis L, Zicha J, Kunes J, Hojna S, Behuliak M, Celec P, Kojsova S, Pechanova O, Simko F. Regression of L-NAME-induced hypertension: The role of nitric oxide and endothelium-derived constricting factor. *Hypertens Res.* 2008; 31:793–803. [PubMed: 18633192]
35. McCarron JG, Olson ML, Chalmers S. Mitochondrial regulation of cytosolic  $\text{Ca}^{2+}$  signals in smooth muscle. *Pflugers Archiv: European journal of physiology.* 2012; 464:51–62. [PubMed: 22555917]
36. Demaurex N, Poburko D, Frieden M. Regulation of plasma membrane calcium fluxes by mitochondria. *Biochim Biophys Acta.* 2009; 1787:1383–1394. [PubMed: 19161976]
37. Ben-Johny M, Yue DT. Calmodulin regulation (calmodulation) of voltage-gated calcium channels. *The Journal of general physiology.* 2014; 143:679–692. [PubMed: 24863929]
38. McCarron JG, Muir TC. Mitochondrial regulation of the cytosolic  $\text{Ca}^{2+}$  concentration and the  $\text{InsP}_3$ -sensitive  $\text{Ca}^{2+}$  store in guinea-pig colonic smooth muscle. *J Physiol.* 1999; 516:149–161. [PubMed: 10066930]
39. Woo HA, Yim SH, Shin DH, Kang D, Yu DY, Rhee SG. Inactivation of peroxiredoxin I by phosphorylation allows localized  $\text{H}_2\text{O}_2$  accumulation for cell signaling. *Cell.* 2010; 140:517–528. [PubMed: 20178744]
40. Griendling KK, Minieri CA, Ollerenshaw JD, Alexander RW. Angiotensin II stimulates NADH and NADPH oxidase activity in cultured vascular smooth muscle cells. *Circ Res.* 1994; 74:1141–1148. [PubMed: 8187280]
41. Touyz RM, Schiffrin EL. Signal transduction mechanisms mediating the physiological and pathophysiological actions of angiotensin II in vascular smooth muscle cells. *Pharmacol Rev.* 2000; 52:639–672. [PubMed: 11121512]
42. Cheranov SY, Jaggar JH. TNF- $\alpha$  dilates cerebral arteries via NAD(P)H oxidase-dependent  $\text{Ca}^{2+}$  spark activation. *American journal of physiology. Cell physiology.* 2006; 290:C964–971. [PubMed: 16267103]
43. Xi Q, Cheranov SY, Jaggar JH. Mitochondria-derived reactive oxygen species dilate cerebral arteries by activating  $\text{Ca}^{2+}$  sparks. *Circ Res.* 2005; 97:354–362. [PubMed: 16020754]
44. Rajagopalan S, Kurz S, Münzel T, Tarpey M, Freeman BA, Griendling KK, Harrison DG. Angiotensin II-mediated hypertension in the rat increases vascular superoxide production via membrane NADH/NADPH oxidase activation. Contribution to alterations of vasomotor tone. *J Clin Invest.* 1996; 97:1916–1923. [PubMed: 8621776]
45. Török J. Participation of nitric oxide in different models of experimental hypertension. *Physiological research/Academia Scientiarum Bohemoslovaca.* 2008; 57:813–825. [PubMed: 19154086]
46. Nickel A, Kohlhaas M, Maack C. Mitochondrial reactive oxygen species production and elimination. *J Mol Cell Cardiol.* 2014; 73:26–33. [PubMed: 24657720]
47. Viola HM, Arthur PG, Hool LC. Transient exposure to hydrogen peroxide causes an increase in mitochondria-derived superoxide as a result of sustained alteration in L-type  $\text{Ca}^{2+}$  channel function in the absence of apoptosis in ventricular myocytes. *Circulation research.* 2007; 100:1036–1044. [PubMed: 17347474]
48. Zorov DB, Filburn CR, Klotz LO, Zweier JL, Sollott SJ. Reactive oxygen species (ROS)-induced ROS release: A new phenomenon accompanying induction of the mitochondrial permeability transition in cardiac myocytes. *J Exp Med.* 2000; 192:1001–1014. [PubMed: 11015441]
49. Dang AK, Murtazina DA, Magee C, Navratil AM, Clay CM, Amberg GC. GnRH evokes localized subplasmalemmal calcium signaling in gonadotropes. *Mol Endocrinol.* 2014; 28:2049–2059. [PubMed: 25333516]



## Novelty and Significance

### What Is Known?

- Angiotensin II (Ang II) is a clinically targeted endogenous vasoconstrictor implicated in the development of cardiovascular diseases including hypertension and congestive heart failure.
- In arterial smooth muscle, Ang II receptor activation promotes localized reactive oxygen species (ROS) generation by NADPH oxidase which is associated with colocalized calcium ( $\text{Ca}^{2+}$ ) influx through L-type  $\text{Ca}^{2+}$  channels.
- Mitochondria are also a source of ROS generation and are known to integrate  $\text{Ca}^{2+}$  and ROS signaling pathways in many cells.

### What New Information Does This Manuscript Contribute?

- Mitochondria residing near the plasma membrane of rat cerebral arterial smooth muscle cells are associated with sites of elevated  $\text{Ca}^{2+}$  influx through L-type  $\text{Ca}^{2+}$  channels.
- Following Ang II exposure, subplasmalemmal mitochondria amplify localized ROS (hydrogen peroxide) production initiated by NADPH oxidase in signaling microdomains resulting in protein kinase C-dependent activation of neighboring L-type  $\text{Ca}^{2+}$  channels.
- This mitochondrial ROS-dependent stimulation of L-type  $\text{Ca}^{2+}$  channels contributes to contraction of rat cerebral arteries by Ang II.
- Disrupting mitochondrial ROS production in vivo normalizes arterial function and attenuates the hypertensive response to pharmacologically-induced systemic endothelial dysfunction.

Mitochondria are a major source of cellular ROS. In addition, mitochondrial dysfunction is associated with cardiovascular disease. However, the importance of mitochondrial ROS in Ang II-dependent arterial contraction and in hypertension-associated arterial dysfunction is unclear. In this study we tested the hypothesis that mitochondrial ROS generation regulates the activity of L-type  $\text{Ca}^{2+}$  channels in rat cerebral arterial smooth muscle in the context of Ang II signaling. Using an image-based approach, we found that mitochondrial amplification of ROS (hydrogen peroxide) signaling near the plasma membrane stimulates L-type  $\text{Ca}^{2+}$  channels. By providing a means of increased  $\text{Ca}^{2+}$  influx, this mechanism contributes to Ang II-dependent arterial contraction. Our data also show that disrupting this mitochondrial amplification mechanism in vivo normalizes arterial function and attenuates the hypertensive response to systemic endothelial dysfunction. From these observations, we conclude that mitochondrial amplification of hydrogen peroxide signaling leads to increased  $\text{Ca}^{2+}$  influx through L-type  $\text{Ca}^{2+}$  channels. We suggest that this mechanism plays an important role in arterial smooth muscle physiology and contributes to arterial dysfunction in hypertension. We also propose that mitochondrial amplification of ROS signaling in arterial smooth muscle is a



potentially viable therapeutic target for reducing hypertension-associated arterial dysfunction.

Author Manuscript

Author Manuscript

Author Manuscript

Author Manuscript

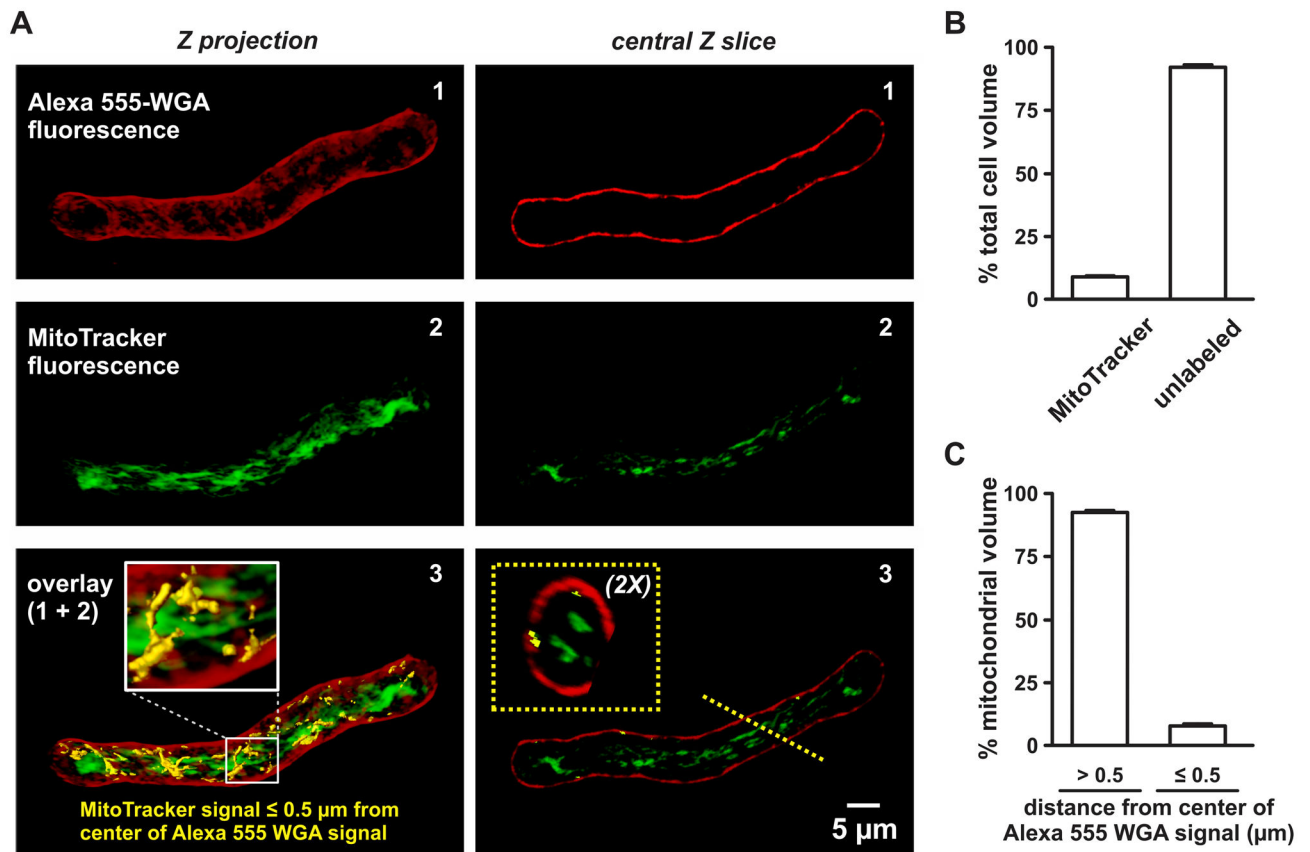


**Figure 1. Subplasmalemmal mitochondria are present but sparse in rat cerebral arterial smooth muscle cells**

**A**, Representative confocal images showing the plasma membrane (Alexa 555-WGA fluorescence, red) and mitochondria (MitoTracker fluorescence, green) in an isolated rat cerebral arterial smooth muscle cell. In panel 3, subplasmalemmal mitochondria ( $< 0.5 \mu\text{m}$  from the plasma membrane) are highlighted yellow. The inset in panel 3 shows *z* projections at the *x* and *y* positions indicated by the dashed yellow lines. **B**, Plot of the mean $\pm$ SEM mitochondrial and non-mitochondrial volumes (% of total cell volume;  $n=5$  cells). **C**, Plot of the mean $\pm$ SEM non-peripheral ( $>0.5 \mu\text{m}$  from the plasma membrane) and subplasmalemmal ( $< 0.5 \mu\text{m}$ ) mitochondrial volumes (% total mitochondrial volume;  $n=5$  cells).

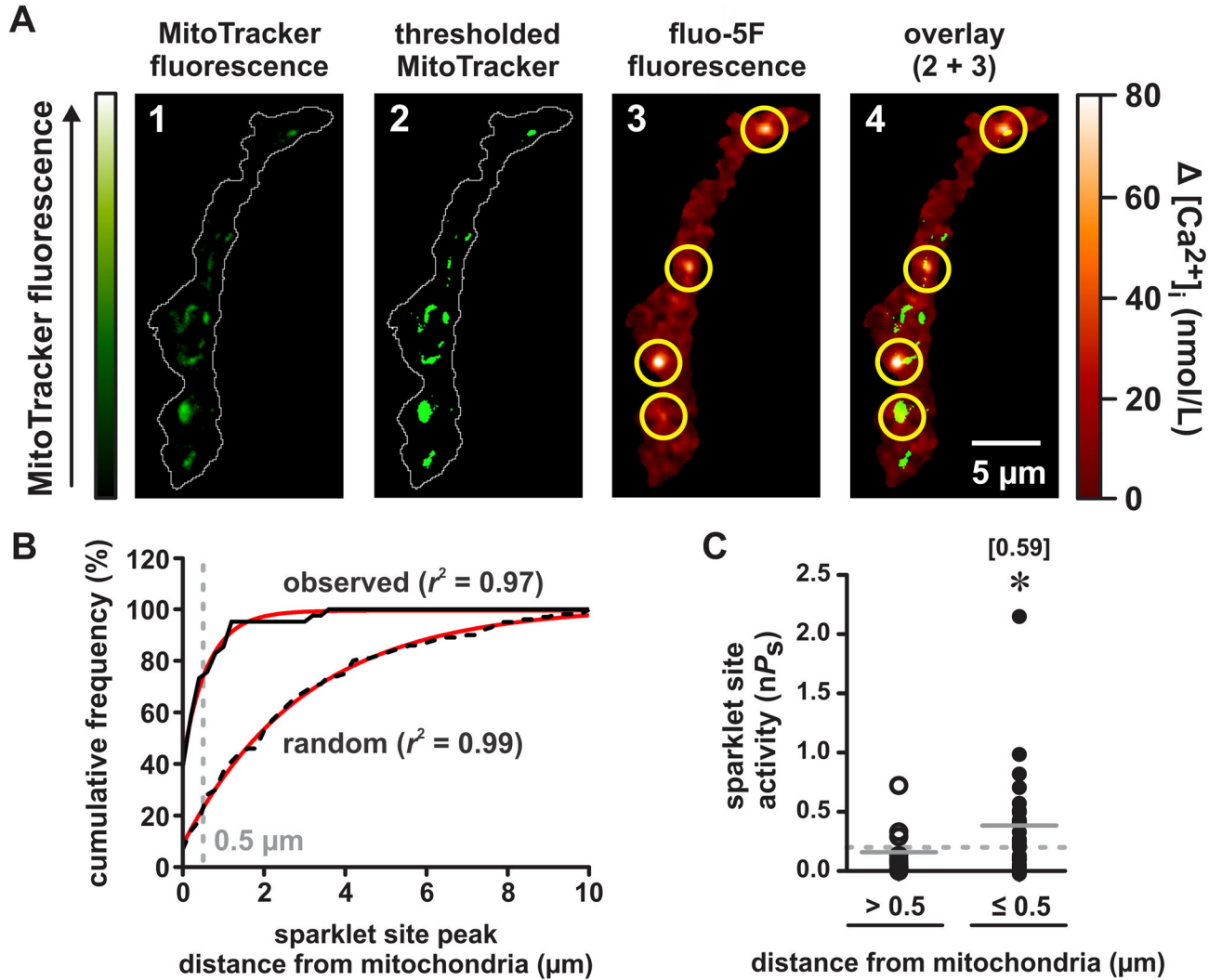


**Figure 2. Active L-type  $Ca^{2+}$  channels associate with subplasmalemmal mitochondria**  
**A**, Representative TIRF images showing subplasmalemmal mitochondria (MitoTracker fluorescence, panel 1; thresholded MitoTracker fluorescence, panel 2), L-type  $Ca^{2+}$  channel-mediated  $Ca^{2+}$  influx (fluo-5F fluorescence; panel 3), and an overlay of panels 2 & 3 (panel 4). Yellow circles in panels 3 and 4 indicate sites of *bone fide* L-type  $Ca^{2+}$  channel sparklet activity (see Online Methods). **B**, Euclidean distance mapping showing cumulative distribution functions representing the distance of observed  $Ca^{2+}$  sparklet site peaks from mitochondria (solid black line;  $n=7$  cells) and from 100 randomly distributed points within visible TIRF footprint (dashed black line). Solid red lines are best fits of the cumulative distributions with a single exponential function as described in the Online Methods. The vertical dashed grey line marks the distance separating mitochondrial associated ( $\leq 0.5 \mu\text{m}$ ) and non-associated ( $>0.5 \mu\text{m}$ )  $Ca^{2+}$  sparklet sites. **C**, Plot of  $Ca^{2+}$  sparklet site activities ( $nP_s$ , where  $n$  is the number of quantal levels detected and  $P_s$  is the probability that the site is active) at sites  $>0.5 \mu\text{m}$  and  $\leq 0.5 \mu\text{m}$  from the nearest thresholded MitoTracker signal ( $n=5$  cells). The horizontal dashed grey line marks the threshold for high-activity  $Ca^{2+}$

sparklet sites ( $nP_s$  0.2; see Online Methods). Bracketed values indicate effect size ( $r$ ).  
\* $P < 0.05$

Author Manuscript

Author Manuscript

Author Manuscript

Author Manuscript

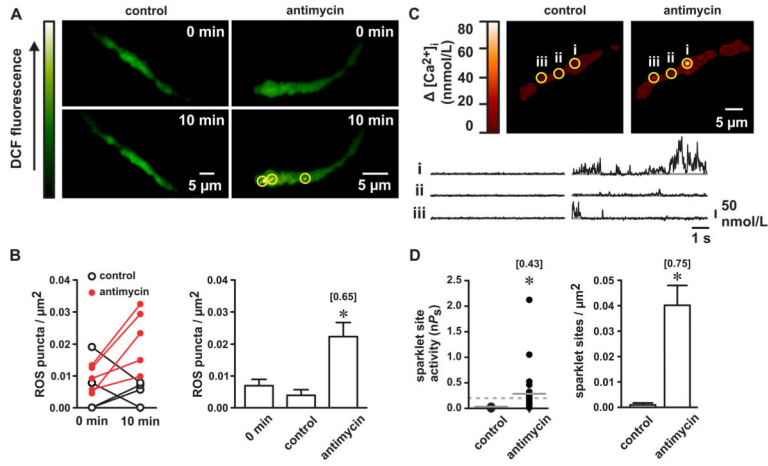


**Figure 3. ROS generation by subplasmalemmal mitochondria is punctate and stimulates L-type Ca<sup>2+</sup> channels**

**A**, Representative TIRF images showing subplasmalemmal DCF fluorescence (indicating intracellular oxidation) in a control cell (*left*) and in a cell incubated with the mitochondrial electron transport chain complex III inhibitor antimycin (500 nmol/L; *right*) at the times indicated. Yellow circles indicate sites of *bone fide* ROS puncta formation (see Online Methods). **B**, Plot of individual ROS puncta densities in control cells (open circles; n=5 cells) and cells treated with antimycin (filled red circles; n=5 cells) at 0 min and at 10 min (*left*) and plot of mean±SEM ROS puncta densities at 0 min (all values) and at 10 min in control and antimycin-treated cells (*right*). **C**, Representative TIRF images showing Ca<sup>2+</sup> influx in a cell before and after application of antimycin (500 nmol/L). Traces show the time course of Ca<sup>2+</sup> influx at the 3 circled sites. **D**, Plot of Ca<sup>2+</sup> sparklet site activities (nP<sub>s</sub>) and plot of mean±SEM Ca<sup>2+</sup> sparklet densities (Ca<sup>2+</sup> sparklet sites/μm<sup>2</sup>) before and after antimycin (n=5 cells). Bracketed values indicate effect size (*r*). \*P<0.05

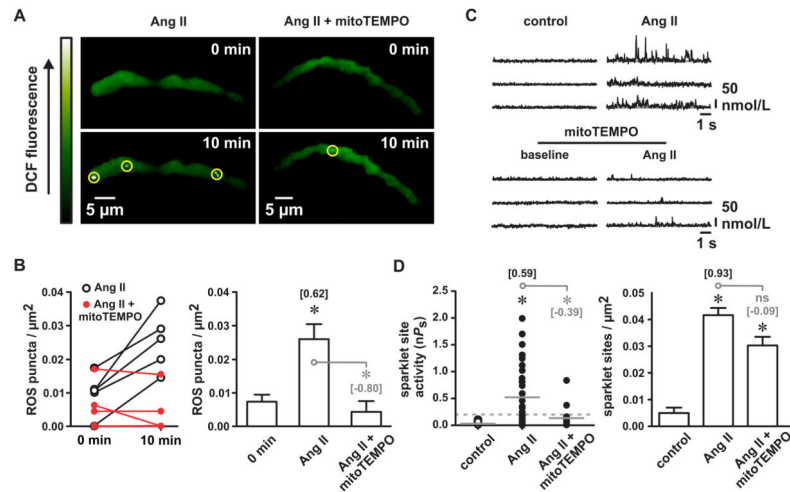


**Figure 4. Mitochondria contribute to angiotensin II-dependent ROS and  $\text{Ca}^{2+}$  microdomain signaling**

**A**, Representative TIRF images showing subplasmalemmal DCF fluorescence in a cell before and after application of Ang II (100 nmol/L; *left*) and in a cell before and after Ang II in the presence of the mitochondrial targeted antioxidant mitoTEMPO (25 nmol/L; *right*). Yellow circles indicate sites of ROS puncta formation. **B**, Plot of individual ROS puncta densities in cells exposed to Ang II (open circles;  $n=5$  cells) and cells exposed to Ang II in the presence of mitoTEMPO (filled red circles;  $n=5$  cells) at 0 min and at 10 min (*left*) and the plot of mean $\pm$ SEM ROS puncta densities at 0 min (all values) and at 10 min in Ang II and Ang II in the presence of mitoTEMPO (*right*). **C**, Representative traces showing time courses of  $\text{Ca}^{2+}$  influx in cells before and after application of Ang II (100 nmol/L) in control cells and in the presence of the mitochondrial targeted antioxidant mitoTEMPO (25 nmol/L). **D**, Plots showing  $\text{Ca}^{2+}$  sparklet site activities ( $nP_s$ ) and mean $\pm$ SEM  $\text{Ca}^{2+}$  sparklet densities ( $\text{Ca}^{2+}$  sparklet sites/ $\mu\text{m}^2$ ) before after Ang II in control cells and in the presence of mitoTEMPO ( $n=5$  cells each). Bracketed values indicate effect size ( $r$ ).  $*P<0.05$

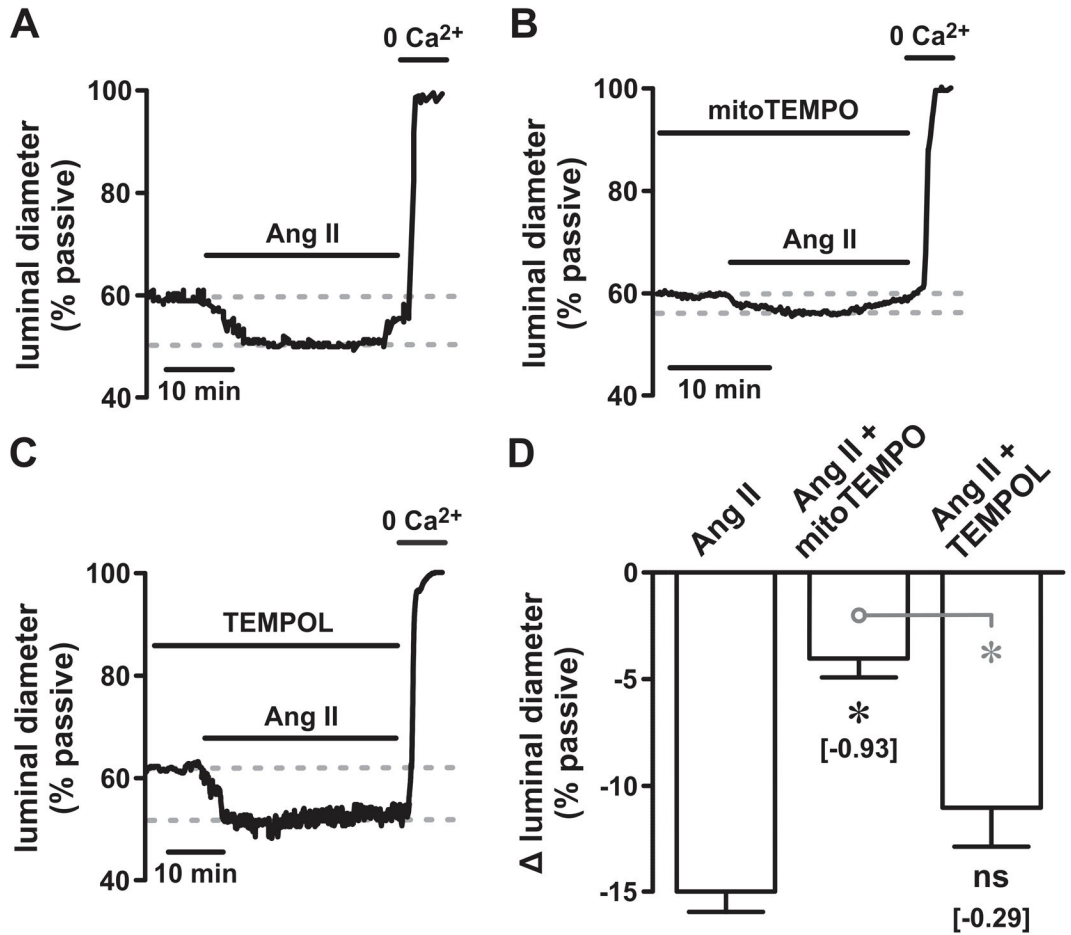


**Figure 5. Smooth muscle mitochondrial ROS contribute to angiotensin II-dependent arterial contractions**

**A–C,** Representative time courses showing luminal diameters (as % passive diameter) of pressurized (60 mmHg) middle cerebral arterial segments exposed to Ang II (10 nmol/L) in the absence (**A**) or presence of the mitochondrial-targeted antioxidant mitoTEMPO (1  $\mu\text{mol/L}$ ) (**B**) or the non-targeted antioxidant TEMPOL (10  $\mu\text{mol/L}$ ) (**C**). The horizontal dashed grey lines represent approximate points of measurement for analysis. **D,** Plot of the mean  $\pm$  SEM induced contraction (% passive diameter) by Ang II in the absence or presence of mitoTEMPO or TEMPOL (n=5 arteries each). Bracketed values indicate effect size (r).

\* $P < 0.05$



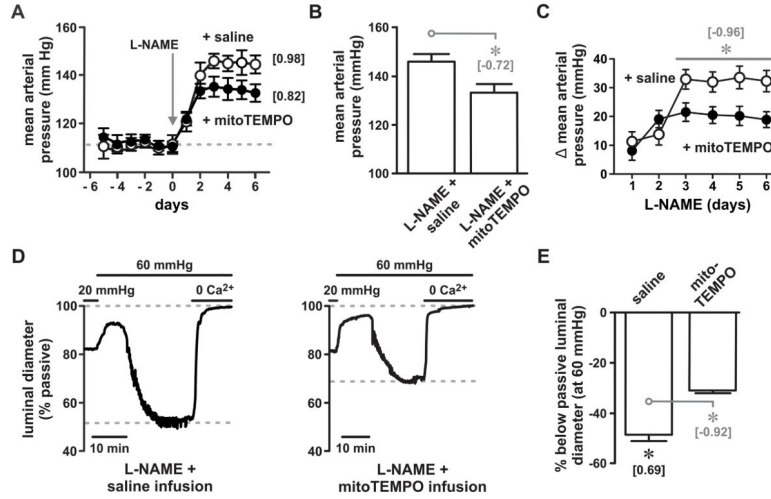


**Figure 6. Arterial smooth muscle mitochondrial ROS contribute to hypertension-associated arterial dysfunction**

**A**, Time courses of mean arterial pressures in rats treated with the nitric oxide synthase inhibitor L-NAME and infused with saline (open circles) or infused with the mitochondrial targeted antioxidant mitoTEMPO (closed circles). **B**, Plot of the terminal mean arterial pressures (mean±SEM) for rats treated with L-NAME and infused with saline or with mitoTEMPO (n=5 rats each). **C**, Time courses of the change in mean arterial pressure in response to L-NAME for rats infused with saline or with mitoTEMPO (n=5 rats each). **D**, Representative time courses showing luminal diameters (as % passive diameter) of pressurized middle cerebral arterial segments (as indicated) isolated from rats treated with L-NAME and infused with saline (*left*) or with mitoTEMPO (*right*). The horizontal dashed grey lines represent approximate points of measurement for analysis. **E**, Plot of the mean ±SEM contraction induced by increasing the intraluminal pressure (20 to 60 mmHg) of middle cerebral arterial segments isolated from rats treated with L-NAME and infused with saline or with mitoTEMPO (n=5 arteries each). Bracketed values indicate effect size (*r*). \**P*<0.05

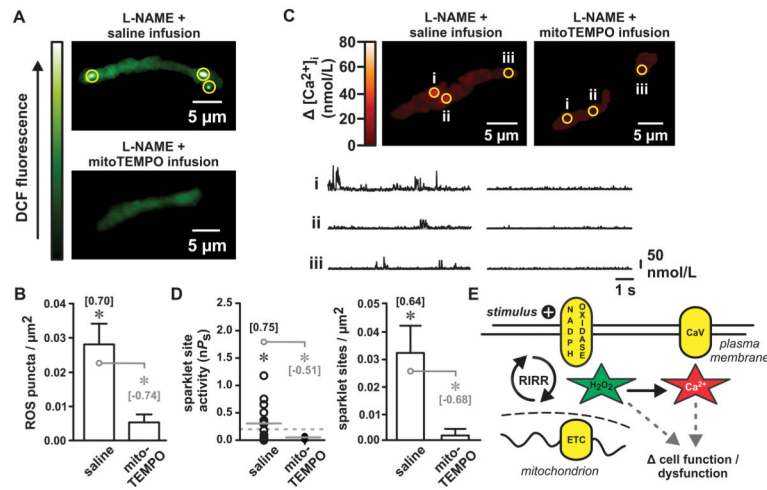


**Figure 7. Endothelial dysfunction increases arterial smooth muscle mitochondrial ROS and  $\text{Ca}^{2+}$  microdomain signaling**

**A**, Representative TIRF images showing subplasmalemmal DCF fluorescence in a cell isolated from rats treated with the nitric oxide synthase inhibitor L-NAME and infused with saline (*top*) or infused with the mitochondrial targeted antioxidant mitoTEMPO (*bottom*). Yellow circles indicate sites of ROS puncta formation. **B**, Plot of mean $\pm$ SEM ROS puncta densities in cells isolated from rats treated with L-NAME and infused with saline or infused with mitoTEMPO (n=5 cells). **C**, Representative TIRF images showing  $\text{Ca}^{2+}$  influx in cells isolated from rats treated with L-NAME and infused with saline (*left*) or infused with mitoTEMPO (*right*). Traces show the time course of  $\text{Ca}^{2+}$  influx at the 3 circled sites. **D**, Plot of  $\text{Ca}^{2+}$  sparklet site activities ( $nP_s$ ) and plot of mean $\pm$ SEM  $\text{Ca}^{2+}$  sparklet site densities ( $\text{Ca}^{2+}$  sparklet sites/ $\mu\text{m}^2$ ) in cells isolated from rats treated with L-NAME and infused with saline or infused with mitoTEMPO (n=5 cells). Black asterisks and effect sizes in panels B and D are in reference to non-L-NAME-treated controls. **E**, Proposed mechanism where mitochondrial ROS-induced ROS release (RIRR) amplifies  $\text{H}_2\text{O}_2$  microdomain signaling leading to stimulation of colocalized  $\text{Ca}^{2+}$  influx through L-type  $\text{Ca}^{2+}$  channels resulting in changes ( ) in cell function or induction of cell dysfunction. CaV=L-type  $\text{Ca}^{2+}$  channel; ETC=mitochondrial electron transport chain. Bracketed values indicate effect size (r). \* $P<0.05$